

Comprehensive analysis of blood group antigen binding to classical and El Tor cholera toxin B-pentamers by NMR

Journal:	<i>Glycobiology</i>
Manuscript ID:	GLYCO-2014-00033.R1
Manuscript Type:	Regular Manuscripts
Date Submitted by the Author:	n/a
Complete List of Authors:	Vasile, Francesca; Universita' degli Studi di Milano, Dipartimento di Chimica Reina, José J; Universita' degli Studi di Milano, Dipartimento di Chimica Potenza, Donatella; Universita' degli Studi di Milano, Dipartimento di Chimica Heggelund, Julie Elisabeth; University of Oslo, Department of Chemistry Mackenzie, Alasdair; University of Oslo, Department of Chemistry Krengel, Ute; University of Oslo, Chemistry Bernardi, Anna; Universita' degli Studi di Milano, Dipartimento di Chimica
Key Words:	ABH blood group determinants , binding affinity , cholera blood group dependence, nuclear magnetic resonance spectroscopy (STD and tr- NOESY), cholera toxin

1
2
3 **Comprehensive analysis of blood group antigen binding to**
4
5 **classical and El Tor cholera toxin B-pentamers by NMR**
6
7

8 *Francesca Vasile,^a José J. Reina,^a Donatella Potenza,^a Julie E. Heggelund,^b Alasdair*
9
10 *Mackenzie,^{b,c} Ute Krengel,^b Anna Bernardi^a*
11

12
13
14
15 ^aUniversita' degli Studi di Milano, Dipartimento di Chimica, via Golgi 19, 20133
16
17 Milano, Italy

18
19 ^bUniversity of Oslo, Department of Chemistry, P.O. Box 1033, Blindern, NO-0315,
20
21 Norway
22

23
24 ^cPresent address: Department of Chemistry, Biotechnology and Food Science,
25
26 Norwegian University of Life Sciences, P.O.Box 5003, NO-1432 Ås, Norway
27

28
29
30
31
32
33 Correspondence should be addressed to A.B. (anna.bernardi@unimi.it), Tel.:+39
34
35 0250314092 , Fax: +39 0250314092 and U. K. (ute.krengel@kjemi.uio.no), Tel.: +47
36
37 22 85 54 61, Fax: +47 22 85 54 41
38

39
40
41
42 **Running Title:** NMR study of blood group antigen binding to cholera toxin
43

44
45
46 **Supplementary data:** Chemical shift assignment of blood group analogs **1b-3b**;
47
48 NOESY studies: conformational analysis; STD amplification factors and calculation
49
50 of binding constants
51
52
53
54
55
56
57
58
59
60

1
2
3 **Keywords:** ABH blood group determinants / binding affinity / cholera blood group
4
5 dependence / nuclear magnetic resonance spectroscopy (STD and tr-NOESY) /
6
7 cholera toxin
8
9
10
11
12
13
14
15
16
17
18
19
20
21
22
23
24
25
26
27
28
29
30
31
32
33
34
35
36
37
38
39
40
41
42
43
44
45
46
47
48
49
50
51
52
53
54
55
56
57
58
59
60

For Peer Review

ABSTRACT

Cholera is a diarrheal disease responsible for the deaths of thousands, possibly even hundreds of thousands of people every year, and its impact is predicted to further increase with climate change. It has been known since decades that blood group O individuals suffer more severe symptoms of cholera compared to individuals with other blood groups (A, B, AB). The observed blood group dependence is likely to be caused by the major virulence factor of *Vibrio cholerae* the cholera toxin. Here, we investigate the binding of ABH blood group determinants to both classical and El Tor cholera toxin B-pentamers using STD-NMR, and show that all three blood group determinants bind to both toxin variants. Although the details of the interactions differ, we see no large differences between the two toxin genotypes, and observe very similar binding constants. We also show that the blood group determinants bind to a site distinct from that of the primary receptor, GM1. Tr-NOESY data confirm that the conformations of the blood group determinants in complex with both toxin variants are similar to those of reported X-ray and solution structures. Taken together, this detailed analysis provides a framework for the interpretation of the epidemiological data linking the severity of cholera infection and individual's blood group and brings us one step closer to understanding the molecular basis of cholera blood group dependence.

INTRODUCTION

Cholera is a life threatening disease caused by the pathogenic bacterium *Vibrio cholerae*. The disease is caused by a secreted protein, the cholera toxin (CT), which consists of a heterohexamer formed by one toxic A-subunit (CTA) anchored in the middle of a ring formed by five B-subunits (CTB). The B-pentamer is responsible for targeting the toxin to human intestinal epithelial cells by binding to the GM1 ganglioside (Gal β 3GalNAc β 4[NeuAc α 3]Gal β 4Glc β Cer) present on their surface. Binding of the toxin results in its internalization, and the release of the CTA subunit, which through a cascade of events ultimately leads to extreme diarrhea, and if untreated, death as a result of such rapid dehydration. The two major biotypes of cholera are Classical and El Tor, which produce toxins that typically differ only by two residues in their B-subunits at positions 18 and 47 (Y18 and I47 in El Tor, H18 and T47 in classical CTB) (Sánchez and Holmgren 2008)

The severity of cholera symptoms, particularly for the El Tor biotype, has been reported to depend upon the patient's blood group (Clemens, Sack, et al. 1989, Harris, Khan, et al. 2005, Harris, LaRocque, et al. 2008). Blood type is, in part, determined by the ABH antigens, oligosaccharides expressed on cell surfaces, including those of the gastro-intestinal tract. These three antigens define the blood groups A, B and O, respectively. They contain a common 2-*O*-fucosyl-galactoside structure (as in H-tetrasaccharide **1**, Figure 1), which is further substituted towards the non-reducing end by an α -galactosamine residue (in A-pentasaccharide **2**, Figure 1) or an α -galactose (in B-pentasaccharide **3**, Figure 1). Blood group O individuals, carrying the H-antigen, appear to be more at risk of developing severe cholera than those of other blood groups (Barua and Paguio 1977, Chaudhuri and De 1977, Glass, Holmgren, et al. 1985, Swerdlow, Mintz, et al. 1994). This appears to be related to the toxin B-

1
2
3 pentamer structure. Previous crystallographic studies revealed a secondary binding
4
5 site in a CTB homolog, the human heat-labile enterotoxin from *Escherichia coli*
6
7 (hLTB) (Holmner, Askarieh, et al. 2007) as well as in a CTB/hLTB chimera
8
9 (Holmner, Lebens, et al. 2004), which was able to interact with blood group
10
11 oligosaccharides. These structural investigations showed the A type 2-antigen analog
12
13 **2b** (Figure 1) binding to the toxin B-pentamers in a region which includes residues 18
14
15 and 47 (Y18 and T47 in hLTB and in the CTB/hLTB chimera). In the crystal
16
17 structures, the Tyr18 hydroxyl group was found to exhibit strong van der Waals
18
19 interactions with the reducing end Glc β of **2b**, and to coordinate a conserved water
20
21 network at this site (Holmner, Lebens, et al. 2004). This suggested that the El Tor
22
23 CTB (possessing Y18) could be capable of stronger interactions with the blood group
24
25 antigens compared to the classical CTB (possessing H18), which would provide a
26
27 possible explanation as to the stronger blood group dependence of El Tor cholera
28
29 observed by Clemens *et al* (Clemens, Sack, et al. 1989). However, more recently, we
30
31 have reported preliminary studies performed using Surface Plasmon Resonance (SPR)
32
33 and NMR spectroscopy showing that both El Tor and classical cholera toxin B-
34
35 pentamers bind blood group determinants H and A with similar affinities, although
36
37 with different kinetics (Heggelund, Haugen, et al. 2012). Concurrently, Turnbull and
38
39 coworkers (Mandal, Branson, et al. 2012) reported isothermal titration calorimetry
40
41 (ITC) and NMR studies for the interaction of β -glycosides of H- and B-antigen
42
43 analogs **1a** and **3a**, with El Tor CTB and hLTB, showing that the H-antigen analog
44
45 binds to both El Tor CTB and hLTB. Surprisingly, the B-antigen analog **3a** was found
46
47 to bind only to hLTB but not to El Tor CTB. However, a single point mutation at
48
49 position 47 in El Tor CTB (I47T) restored the B-antigen-binding activity of the
50
51 protein, which suggested a strong role for this residue in the interaction.
52
53
54
55
56
57
58
59
60

1
2
3 Here we report a comprehensive analysis using STD NMR and tr-NOESY
4 experiments (Dalvit 2009, Meyer and Peters 2003) to examine the interactions of
5 classical CTB and El Tor CTB with analogs of all three blood group determinants H-
6 tetra, A-penta and B-penta (compounds **1b**, **2b** and **3b** respectively, Figure 1). In all
7 cases, the STD spectra showed clear interactions with both proteins, and indicated
8 that each oligosaccharide binds to the two different CTB pentamers in a similar
9 orientation. We observed some small but significant differences in the atomic details
10 of the interaction of the three antigen analogs with either El Tor or classical CTB, but
11 the estimated K_d values for the complexes are very similar. The tr-NOESY data
12 support a binding conformation consistent with that observed in the X-ray structure of
13 the A-antigen analog **2b** bound to hLTB (Holmner, Askarieh, et al. 2007). In addition,
14 we have shown, through competition experiments, that the blood group H-
15 tetrasaccharide **1b** and the GM1 oligosaccharide (GM1-os, **4**, Figure 1) bind at
16 different sites on classical CTB, as already suggested by Mandal *et al.* for El Tor CTB
17 (Mandal, Branson, et al. 2012). Thus, this work offers a comprehensive frame for
18 interpretation of the epidemiological analysis linking CT infection and blood type.
19
20
21
22
23
24
25
26
27
28
29
30
31
32
33
34
35
36
37
38
39
40
41
42
43
44
45
46
47
48
49
50
51
52
53
54
55
56
57
58
59
60

RESULTS

The interaction of **1b-3b** (Figure 1) with CTB was studied by STD-NMR and tr-NOESY. Saturation Transfer Difference NMR (STD-NMR) is one of the most used NMR methods to study the interactions between oligosaccharides and macromolecular receptors (Bhunja, Bhattacharjya, et al. 2012, Meyer and Peters 2003). The technique helps identifying the epitope group of the ligands, revealing which moieties are closest to the receptor in the bound state. It is based on the transfer of magnetization from the protein to the bound ligand, which, by exchange, is released into solution where it is detected. The degree of saturation of individual ligand protons (expressed as absolute-STD percentage) reflects their proximity to the protein surface and can be used to describe the ligand-target interactions.

In addition to epitope mapping, K_d values can be estimated from STD-NMR experiments. In fact, the STD intensity, which depends on the fraction of bound ligand, can be converted into the STD amplification factor (STD-AF), which is a function of the fraction of bound protein (Mayer and Meyer 1999, Mayer and Meyer 2001). The evolution of the STD-AF along a ligand titration series enables the construction of a saturation curve and the value of K_d results from mathematical fitting of the experimental curve.

An NMR spectroscopic technique complementary to STD is transferred NOESY (tr-NOESY) (Haselhorst, Espinosa, et al. 1999, Mayer and Meyer 2000, Meyer, Weimar, et al. 1997, Post 2003). The observation of tr-NOEs relies on the different behavior of a small ligand molecule free in solution, rather than bound to a receptor protein. A ligand bound to a large molecular weight protein behaves as part of the large molecule, and adopts the corresponding NOE behavior, showing strong negative NOEs, so-called tr-NOEs. Binding of a ligand to a receptor protein can thus easily be

1
2
3 distinguished by looking at the sign of the observed NOEs. These tr-NOEs reflect the
4
5 bound conformation of the ligand, so that data can be inferred about the
6
7 conformational equilibrium of the ligand during the binding event.
8
9

10 11 ***Ligand interaction studies by STD and ¹H-NMR***

12
13 The complete ¹H- and ¹³C-NMR spectral assignments of free compounds **1b-3b** are
14
15 provided in the *Supplementary Information* (Table S1). All compounds are present as
16
17 an equilibrium α/β anomeric mixture of the reducing end glucose. The STD-NMR
18
19 experiments were performed on soluble classical and El Tor CTB in the presence of
20
21 antigen analogs **1b-3b** in phosphate buffer at 298 K. STD spectra of the ligands in the
22
23 absence of the cholera toxin B-pentamers did not show any signals. However, when
24
25 the ligand complexes were analyzed, only signals resulting from the transfer of
26
27 saturation from the protein receptor to the ligand protons were observed, thus
28
29 permitting immediate mapping of the epitope. In all cases, clear binding was observed
30
31 (see below) and binding constants could be determined from STD growth curves
32
33 (Meyer and Peters 2003). Only one saturation time was selected for the data analysis,
34
35 which allows only for a qualitative determination of binding epitopes. Indeed, the
36
37 STD NMR spectra showed rather low intensities that precluded a more quantitative
38
39 approach using STD build-up curves, to avoid effects of different relaxation times
40
41 (Mayer and James 2004) and rebinding effects (Angulo, Diaz, et al 2008). However,
42
43 the comparative nature of this study, both in terms of carbohydrate ligands and
44
45 protein biotypes, supports the relevance of the qualitative approach used here.
46
47
48
49

50
51 The absolute STD values obtained for **1b-3b** in the presence of classical CTB (cCTB)
52
53 and El Tor (ET CTB) are shown in Figure 2. STD values of overlapping signals were
54
55 not included. In all cases, the highest STD signal was obtained for the anomeric
56
57
58
59
60

1
2
3 proton of the reducing-end glucose. This is most likely an artifact, due to interaction
4
5 with water, and indeed these signals significantly change in intensity, depending on
6
7 the use of water suppression sequences. Therefore, relative STD values were
8
9 calculated for each of the molecules based on the second strongest signal. The relative
10
11 STD values obtained with classical CTB and El Tor CTB are shown in Figure 3. The
12
13 relevant features of the interaction are discussed for each compound in the following
14
15 sections.
16
17

18
19
20
21 *Blood group H tetrasaccharide* $\text{Fu}\alpha\text{2Gal}\beta\text{4}[\text{Fu}\alpha\text{3}]\text{Glc}$ **1b**

22
23 The STD spectrum of H-tetra **1b** in the presence of classical CTB is shown in Figure
24
25 4. Binding involves essentially the protons of the two fucose units, H1-Fuc(I) (5.2
26
27 ppm) and H1-Fuc(II) (5.3 ppm) (Figure 2A and 3). The signals of H2- and H4-Fuc(I)
28
29 and H2- and H4-Fuc(II) also appear in the STD spectrum at 3.7 ppm, but cannot be
30
31 quantified due to overlapping signals and are thus not included in Figure 2A.
32
33

34 The binding constant of H-tetra **1b** to classical CTB was calculated from a titration
35
36 curve acquired by varying the H-tetrasaccharide concentration in the presence of the
37
38 same amount of cCTB, which yielded a $K_d = 2.7 \pm 1.0$ mM.
39
40

41 For El Tor CTB, the interaction with **1b** occurs primarily *via* H1 Fuc(I) (the most
42
43 intense STD signal, 2.5 STD%), but also *via* H1 Fuc(II) (1.5 STD%) (Figure 2a and
44
45 Figure 3), hence the binding strength is reversed between the two fucose residues
46
47 compared to classical CTB. Binding further involves the H3 proton of the glucose
48
49 unit (1.1 STD%), an interaction not observed in the H-tetra/cCTB complex. The
50
51 interaction of El Tor CTB was previously investigated by ITC and NMR by Mandal
52
53 *et al.* for a slightly different H-tetra analog **1a** (Figure 1) containing GlcNAc rather
54
55 than Glc at the reducing end and an alkyl linker (R) covalently attached to the
56
57
58
59
60

1
2
3 anomeric position, yielding a K_d value measured by ITC of 1.8 ± 0.2 mM (Mandal,
4
5 Branson, et al. 2012).
6
7

8
9
10 *Blood group H tetrasaccharide and GM1-os can bind to classical CTB*
11 *simultaneously*
12

13
14 In order to exclude the possibility that the H-tetrasaccharide binds to the classical
15 CTB subunits at the same site as GM1-os (*i.e.* the primary binding site), competition
16 studies were performed both by tr-NOESY and STD experiments. The NOESY
17 spectrum of H-tetra in phosphate buffer shows positive NOE contacts (Figure 5A, red
18 cross peaks). Addition of classical CTB (**1b**/cCTB 20:1) to the solution results in
19 negative NOE contacts in the tr-NOESY spectrum (Figure 5B, black cross peaks),
20 indicating the event of binding and allowing the determination of the bound
21 conformation of the ligand (see below). GM1-os (**4**, 1/1 molar ratio with **1b**) was then
22 added to the mixture, and tr-NOESY spectra were recorded again (Figure 5C). The
23 binding affinity of GM1-os to classical CTB was estimated as 43 nM by ITC
24 (Turnbull, Precious, et al. 2004), suggesting that GM1-os could easily displace the
25 weaker H-tetrasaccharide ligand (K_d in the mM range) if there were competition for
26 the same binding site, as observed before for competitive CTB ligands (Bernardi,
27 Arosio, et al. 2003). The H-tetra cross peaks are negative in Figure 5C, showing that
28 **1b** is not displaced from its binding site by GM1-os, and indicating that both
29 compounds can interact simultaneously with CTB at their respective binding sites.
30 This is supported by the STD spectra performed on the same sample and clearly
31 showing the simultaneous presence of the Fuc anomeric signals of H-tetra **1b** (5.2 and
32 5.3 ppm) and of the H3-NeuAc signal of GM1-os at 1.95 ppm (Figure 6).
33
34
35
36
37
38
39
40
41
42
43
44
45
46
47
48
49
50
51
52
53
54
55
56
57
58
59
60

1
2
3 A titration at different H-tetra concentrations (maintaining a fixed concentration of
4 CTB and GM1-os), yielded a K_d value of 3.0 mM, unchanged from the value
5 measured for the interaction in the absence of GM1-os. This is further evidence that
6 GM1 and blood group antigens bind to CTB at different sites, and corroborates the
7 observations of Mandal *et al.* for **1a**/El Tor CTB (Mandal, Branson, et al. 2012).
8
9

10
11
12
13
14
15
16 *Blood group A pentasaccharide GalNAc α 3[Fuc α 2]Gal β 4[Fuc α 3]Glc **2b***
17

18 Preliminary results investigating the interaction of A-penta **2b** with classical CTB
19 have been reported previously (Heggelund, Haugen, et al. 2012). In brief, the STD
20 spectra of **2b** acquired in the presence of cCTB (Figure 7A,B) indicate that the
21 protons of the oligosaccharide that are more involved in interactions with the toxin are
22 H1-GalNAc, H5-Fuc(II), H1-Fuc(II), H1-Fuc(I) and Ac-GalNAc (2.0, 1.3, 1.1, 1.1
23 and 1.0 absolute STD values, respectively) (Figure 2B). In addition, in the STD
24 spectrum other signals belonging to the GalNAc, Gal, Fuc(I) and Fuc(II) residues
25 appear, although with weaker intensity. The relative STD values, grouped in four
26 intensity ranges, are reported in Figure 3. The titration of A-penta in the presence of
27 43 μ M cCTB yielded a K_d of 5.2 ± 0.8 mM. This value is compatible with the value
28 obtained previously by SPR (1.2 ± 0.3 mM) (Heggelund, Haugen, et al. 2012),
29 especially given that overestimation of dissociation constants is a known feature of
30 STD methods (Angulo, Enríquez-Navas, et al. 2010, Angulo and Nieto 2011).
31
32

33
34
35
36
37
38
39
40
41
42
43
44
45
46
47 A-penta **2b** was also studied in the presence of El Tor CTB (Figure 7B,C). Absolute
48 and relative STD values are shown in Figures 2B and 3. A comparison of the STD
49 spectra acquired for both biotypes suggests that A-penta binds both proteins in a
50 similar fashion, although with several important differences.
51
52
53
54
55
56
57
58
59
60

1
2
3 When comparing the interactions of A-penta **2b** with the toxin B-pentamers of the
4 different biotypes, the STD signals are in general less intense for the **2b**/ El Tor CTB
5 complex compared to the cCTB complex (Figure 2B). Additionally, although the H1-
6 GalNAc proton remains the most intense STD signal in both spectra, all other
7 GalNAc proton signals are missing in the **2b**/ El Tor CTB spectrum. Furthermore, the
8 strong signal observed for H5-Fuc (II)/cCTB is missing in the **2b**/ El Tor CTB
9 spectrum. Despite these atomic-level differences, the K_d value for the the A-penta/ El
10 Tor CTB complex, is 6.4 ± 2.1 mM, very similar to the value for **2b**/cCTB.
11
12
13
14
15
16
17
18
19
20
21
22

23 *Blood group B pentasaccharide Gal α 3[Fuca2]Gal β 4[Fuca3]Glc **3b***

24
25 The STD spectrum of B-penta **3b**, acquired in the presence of classical CTB (Figure
26 8A), shows interactions similar to those observed for the A-antigen analog **2b**,
27 involving principally the two fucose units, the blood group B-specific Gal(II), and the
28 reducing end glucose residue (Figure 2C, 3 and Fig. 8A,B). A titration with increasing
29 concentrations of B-penta in the presence of 43 μ M classical CTB yielded a
30 dissociation constant K_d of 7.2 ± 1.6 mM.
31
32
33
34
35
36
37
38

39 When B-penta was studied in the presence of El Tor CTB, STD signals were also
40 clearly observed (Figure 8C) and absolute values could be quantitatively calculated
41 (Figure 2C). A K_d of 8.1 ± 2.3 mM was obtained, comparable to cCTB. Only minor
42 differences were observed in the spectra for the two CTB variants, with the exception
43 of H2-Glc, which gave a very strong signal for cCTB, but no signal for El Tor CTB,
44 and H3-Fuc(II), which gave a medium intensity signal for cCTB, but no signal for El
45 Tor CTB. Otherwise, most of the absolute and relative STD values are very similar,
46 although generally less intense for El Tor CTB (Figure 2C and 3), except for H1-
47 Gal(II) and H1-Fuc(II), where the opposite pattern was observed. The strongest
48
49
50
51
52
53
54
55
56
57
58
59
60

1
2
3 interactions involve the two fucose units and the galactose residue Gal(II)
4
5 characteristic of blood group B-antigens and, for cCTB, H2-Glc.
6

7
8 The observation made here that both classical and El Tor CTB bind to B-penta is
9
10 consistent with previous preliminary experiments using Surface Plasmon Resonance,
11
12 where B-penta **3b** was found to bind to El Tor CTB (Heggelund, Haugen, et al. 2012),
13
14 although classical CTB was not tested for binding in the previous study. These
15
16 observations are conflicting with a recent report by Turnbull and coworkers, who
17
18 found that the B-pentasaccharide glycoside **3a** does not interact with El Tor CTB,
19
20 except when Ile47 is replaced with Thr47 of the classical sequence (Mandal, Branson,
21
22 et al. 2012).
23
24

25 26 27 ***Conformational studies by tr-NOESY***

28
29 To investigate the bound conformation of **1b-3b**, tr-NOESY experiments were
30
31 performed with both toxins. Details of these studies are described in the
32
33 *Supplementary Information*. In brief, the tr-NOESY spectra obtained in the presence
34
35 of either classical or El Tor CTB were similar to one another and to the spectra of the
36
37 free sugars. The solution conformation of blood group antigens has been studied in
38
39 careful detail (Yuriev, Farrugia, et al. 2005 and references therein; see *Supplementary*
40
41 *Information* for additional references) and it can be described in all cases by one
42
43 major conformer. This is maintained upon binding to either toxin. For B-penta **3b** in
44
45 complex with classical CTB, only one additional NOE contact was observed (H5-
46
47 Fuc(I)/ H2-Gal), indicating that in the bound form, Fucose (I) has a lower degree of
48
49 mobility than in the free form and suggesting the selection of a more rigid
50
51 conformation. For the A-antigen analog **2b**, the conformation supported by tr-NOESY
52
53 experiments corresponds to the one observed in the X-ray structures (PDB ID: 3EFX,
54
55
56
57
58
59
60

1
2
3 Holmner, Lebens, et al. 2004 and PDB ID: 2O2L, Holmner, Askarieh, et al. 2007;
4
5 Figure 9).
6
7
8
9

10 *Summary of interactions - Comparison of cholera biotypes*

11 All three blood group analogs interact with both classical and El Tor cholera toxin B-
12 pentamers, with dissociation constants in the mM range. Despite the two amino acid
13 substitutions (H18Y and T47I; cCTB to El Tor CTB), the binding constants are
14 equivalent within error limits for the two biotypes, with H-tetra **1b** showing the
15 strongest binding, followed by A-penta **2b**, and B-penta **3b** showing the weakest
16 binding.
17
18
19
20
21
22
23

24 The blood group antigen binding site is distinct from the GM1 binding site and
25 presumably corresponds to the binding site identified for the A-analog **2b** in the X-ray
26 crystal structures of hLTB (Holmner, Askarieh, et al. 2007) and the CTB-LTB
27 chimera (Holmner, Lebens, et al. 2004). The two fucose residues are involved in the
28 binding of both biotypes for all three blood group antigens, with the H1 atoms playing
29 a dominant role, whereas the central galactose residue only contributes to the binding
30 of the A- and B-determinants (Figures 2 and 3). The GalNAc and Gal residues
31 characteristic of A- and B-determinants, respectively, are involved in blood group
32 antigen binding independent of the biotype. In each case, however, the intensity,
33 number and exact positions of the STD contacts vary.
34
35
36
37
38
39
40
41
42
43
44
45
46

47 The atomic details of the variations are clearly visible for A-penta GalNAc, which
48 shows multiple STD contacts with cCTB (H1-, H2-, H5-, Ac-GalNAc) and a single
49 contact (H1-GalNAc) with El Tor CTB (Figure 2B). In the crystal structure of **2b** in
50 the CTB/hLTB chimera (Figure 9; PDB ID: 3EFX, Holmner, Lebens, et al. 2004),
51 which like cCTB features a threonine residue at position 47, the GalNAc residue is
52
53
54
55
56
57
58
59
60

1
2
3 positioned near Thr47 and binds to the protein mainly through water-mediated
4 interactions, and through two H-bonds of the GalNAc *N*-acetyl nitrogen to Gly45 O
5 and Thr47 OG1. The lower resolution structure of hLTB (T47) in complex with this
6 ligand (PDB ID: 2O2L, Holmner, Askarieh, et al. 2007) shows the same interactions.
7
8 It is not clear how a substitution of Thr47 for Ile47 in El Tor CTB would affect ligand
9 binding. The substitution of Thr47 for Ile in its preferred rotamer conformation
10 (Figure 9) suggests that small adaptations may be sufficient to accommodate the
11 ligand; on the other hand, Mandal *et al.* observed no binding of this protein variant to
12 a blood group B-determinant (Mandal, Branson, et al. 2012).
13
14

15
16 The STD spectra of **2b** further reveal small differences between the two biotypes in
17 the region of Fuc(II) and, to some extent, Gal. Several contacts, most notably that of
18 H5-Fuc(II), are only observed for one of the protein variants. On the other hand,
19 Fuc(I) and Glc, which in the published crystal structures are in the proximity of
20 residue 18 (Holmner, Askarieh, et al. 2007, Holmner, Lebens, et al. 2004), are not
21 affected. In the CTB/hLTB chimera (PDB ID: 3EFX, Holmner, Lebens, et al. 2004),
22 Y18 coordinates a water network (Figure 9B), which is of significant importance for
23 glucose binding of **2b**. In classical CTB, Y18 is replaced by the smaller H18 which is
24 unlikely to form a similar network. However, this does not necessarily prevent the
25 interaction from occurring.
26
27

28
29 The absolute STD values measured for the fucose residues are essentially the same for
30 A-penta **2b** and B-penta **3b** with either protein (H1-Fuc(I), H6-Fuc(I), H1-Fuc(II),
31 H6-Fuc(II), Figure 2B,C). The signal of H5-Fuc(II), which is strong in the STD
32 spectrum of **2b**, could not be analyzed for B-penta **3b** due to overlapping signals (at
33 4.71 ppm). Some differences between the analogs are associated with the different
34 residues (GalNAc and Gal) at the non-reducing end of each sugar and with the
35
36
37
38
39
40
41
42
43
44
45
46
47
48
49
50
51
52
53
54
55
56
57
58
59
60

1
2
3 terminal Glc H2 proton. Another small difference concerns H3-Fuc(II). It is worth
4
5 repeating that these differences do not lead to major changes in the measured K_d
6
7 values, which are at the upper limit available to the technique.
8
9
10
11
12
13
14
15
16
17
18
19
20
21
22
23
24
25
26
27
28
29
30
31
32
33
34
35
36
37
38
39
40
41
42
43
44
45
46
47
48
49
50
51
52
53
54
55
56
57
58
59
60

For Peer Review

DISCUSSION

In the quest to understand the molecular mechanisms for the observed blood group dependence of cholera, a number of different methods have been used, including protein crystallography (Holmner, Lebens, et al. 2004, Holmner, Askarieh, et al. 2007), NMR (Heggelund, Haugen, et al. 2012, Mandal, Branson, et al. 2012), and quantitative binding studies by SPR (Heggelund, Haugen, et al. 2012) or ITC (Mandal, Branson, et al. 2012). Both classical and El Tor CTB have been investigated, in addition to a CTB/LTB chimera, which contains Tyr18, Thr47 and the CTB-specific residue Asn4 (Holmner, Lebens, et al. 2004). The tested ligands are analogs of the A, B and H blood group determinants A Lewis-y, B Lewis-y and Lewis-y. A and B Lewis-y represent the epitopes on the glycosphingolipids from the human small intestinal epithelium that tested binding-positive in an initial study (Ångström, Bäckström, et al. 2000), and are commonly found in the small intestinal mucosa, especially in secretors (Ravn and Dabelsteen 2000). In our current work, we expanded our investigation of the potential involvement of CTB in the cholera blood group dependence phenomenon using NMR, in particular STD and tr-NOESY. These are very versatile and sensitive methodologies that utilize NOE effects to investigate the interaction between protein and ligand. We confirmed that binding of the blood group oligosaccharides occurs at a site distinct from the primary GM1 binding site, and showed that all three blood group antigen analogs (H-tetra **1b**, A-penta **2b** and B-penta **3b**) bind to the El Tor CTB as well as to classical CTB.

This is in contrast to the recent report by Turnbull and coworkers (Mandal, Branson, et al. 2012), who observed, using STD and ITC, that only a β -glycoside of the H-tetrasaccharide **1a**, but not the corresponding β -glycoside of the B-pentasaccharide **3a** bound to CTB El Tor. This raises the question as to why two studies have produced

1
2
3 such contrasting data for the interaction of the B-antigen interaction with CTB.
4
5 Disregarding any potential technical problems with the STD experiments, the most
6
7 likely cause for the difference is the different oligosaccharides investigated, as the
8
9 recombinant constructs for El Tor CTB were identical (generously provided to us by
10
11 T. Hirst, through the hands of B. Turnbull). The oligosaccharides used in our study
12
13 are from human milk **1b-3b**, which lack the *N*-acetyl group of GlcNAc and are used
14
15 as anomeric mixtures at the reducing end residue. This choice was dictated by the
16
17 commercial availability of compounds in earlier experiments (Holmner, Lebens, et al.
18
19 2004; Holmner, Askarieh, et al. 2007). The Turnbull group employed synthetic
20
21 analogs **1a** and **3a** (Figure 1), which contain the terminal *N*-acetyl group and in
22
23 addition feature a 3-methyloxycarbonylaminopropyl group (R) covalently attached to
24
25 the anomeric position of GlcNAc, locking the anomeric carbon in the β -configuration.
26
27 Non-binding could hence depend either on the additional *N*-acetyl group of GlcNAc
28
29 or on the alkyl linker attached to the anomeric position of the reducing end sugar. The
30
31 published crystal structures do not indicate any potential clash for the *N*-acetyl group,
32
33 which in fact was mistakenly included in the original structural model of the
34
35 CTB/LTB chimera (PDB ID: 3EFX, Holmner, Lebens, et al. 2004). However, this
36
37 structure featured Thr and not Ile at position 47 at the other end of the binding site
38
39 (see Figure 9), and Turnbull and coworkers convincingly showed that they were able
40
41 to restore the binding activity of the El Tor CTB for their B-analog by the substitution
42
43 I47T (Thr being the classical residue) (Mandal, Branson, et al. 2012). The CTB/LTB
44
45 chimera further showed significantly increased binding affinity to blood group A and
46
47 B antigens in microtiter well assays compared to classical CTB (Ångström,
48
49 Bäckström, et al. 2000), which features a histidine residue at position 18. These
50
51 studies, however, were undertaken with glycosphingolipids rather than with blood
52
53
54
55
56
57
58
59
60

1
2
3 group oligosaccharides. Together, these studies suggest that both Tyr18 and Thr47
4
5 correlate with enhanced binding, whereas His18 and Ile47 may correlate with weaker
6
7 binding. The combinations His18/Thr47 and Tyr18/Ile47, as found in classical and El
8
9 Tor CTB, respectively, may then compensate to yield a moderate effect, explaining
10
11 why we obtained virtually identical binding constants for A- and B-penta, to either
12
13 classical CTB or El Tor CTB. *V. cholerae* strains that produce a toxin featuring both
14
15 Tyr18 and Thr47 have also been reported, such as for some O139 Bengal strains
16
17 circulating between 1999 to 2005 (Bhuiyan, Nusrin, et al. 2009), however to the best
18
19 of our knowledge, they have not been analyzed with respect to blood group
20
21 dependence.
22
23

24
25 When comparing the atomic details of binding interactions of the different blood
26
27 group oligosaccharides to the two CTB variants, some differences were observed. For
28
29 B-penta, the main difference in interaction intensity was observed at the reducing end
30
31 of the oligosaccharide, which is expected to bind in the proximity of residue 18 of the
32
33 protein in accordance with previous studies (Holmner, Lebens, et al. 2004, Holmner,
34
35 Askarieh, et al. 2007). It is at the reducing end of the oligosaccharide, where the B-
36
37 antigen analog investigated by us differs from the analog studied by Turnbull and
38
39 coworkers (Mandal, Branson, et al. 2012). For A-penta, the strongest differences were
40
41 found at the non-reducing end, close to residue 47 at the interface to the neighboring
42
43 toxin B-subunit. While the structural changes caused by the amino acid substitutions
44
45 are expected to be small, they may affect the ligand orientation, with consequences
46
47 for ligand interactions at the other end of the binding site. Furthermore, the different
48
49 binding kinetics of A- or B- compared to H-determinants (as seen by SPR;
50
51 Heggelund, Haugen, et al. 2012) suggest that also adjustments of the subunits within
52
53 the B-pentamer might occur, within a delicate balance of binding interactions.
54
55
56
57
58
59
60

1
2
3 In conclusion, the observed interaction of all three blood group antigen analogs tested
4 here (H-tetra, A-penta and B-penta) with both classical and El Tor CTB, provides
5 evidence that also the natural blood group antigens can interact with CTB. Although a
6 trend is clearly visible in the measured K_d (K_d of H-tetra < K_d of A-penta < K_d of B-
7 penta), the small difference in binding affinities for the three blood group
8 determinants is unlikely to cause a large biological effect. We still contend that the
9 blood group dependence associated with cholera severity is likely to occur due to the
10 difference in kinetics as previously reported (Heggelund, Haugen, et al. 2012). At
11 present, we cannot explain why El Tor cholera should show a stronger blood group
12 dependence than the classical disease, but we note that the data excluding classical
13 cholera (Clemens, Sack, et al. 1989) have a small sample size. Furthermore, El Tor
14 strains of *V. cholerae* O1 in Bangladesh have, since 2001, been observed to produce
15 the classical CT genotype (Nair, Qadri, et al. 2006), while blood group dependence is
16 continuing to be reported (Harris, Khan, et al. 2005, Harris, LaRocque, et al. 2008),
17 suggesting that there is no statistically significant difference in blood group
18 dependence between cholera toxin genotypes. The secretor status of the individuals is
19 more likely to be an important determining factor in cholera severity, as the presence
20 of blood group antigens in the mucus layer can have a protective effect against
21 cholera, in particular for blood group A and B individuals (Chaudhuri and
22 DasAdhikary 1978, Arifuzzaman, Ahmed, et al. 2011). A similar effect may underlie
23 the protection conferred by fucosylated human milk oligosaccharides against diarrhea
24 in breastfed infants (Newburg, Ruiz-Palacios, et al. 2004; Blank, Dotz, et al. 2012).
25 Furthermore, with approximately 80% of the normal Indian population being secretor
26 positive (Chaudhuri and DasAdhikary 1978), secretor status is likely to have strongly
27 contributed to shaping the extreme blood group distribution in present Bangladesh. As
28
29
30
31
32
33
34
35
36
37
38
39
40
41
42
43
44
45
46
47
48
49
50
51
52
53
54
55
56
57
58
59
60

1
2
3
4
5
6
7
8
9
10
11
12
13
14
15
16
17
18
19
20
21
22
23
24
25
26
27
28
29
30
31
32
33
34
35
36
37
38
39
40
41
42
43
44
45
46
47
48
49
50
51
52
53
54
55
56
57
58
59
60

the ancestral home of cholera and in addition a region endemic to malaria, which disproportionately affects blood group A individuals, this may explain why Bangladesh exhibits one of the highest incidences of the otherwise rare type B blood allele in the world.

For Peer Review

MATERIALS AND METHODS

The blood group antigen analogs H-tetra, A-penta and B-penta were purchased from Elicityl (catalogue number GLY066, GLY067 and GLY068, respectively).

Protein Production and sample preparation

Lyophilized classical CTB was purchased from Sigma-Aldrich containing Tris buffer salts, NaCl, NaN₃ and Na₂EDTA. The powder was dissolved in D₂O, resulting in classical CTB in 0.05 M Tris buffer, 0.2 M NaCl, 0.003 M NaN₃ and 0.001 M Na₂EDTA, pH 7.5. The signals of Tris and EDTA fall in the same region as the signals of the ligand, so the sample was ultrafiltered using a Millipore Amicon Ultra-4 centrifugal filter unit (MWCO 5,000 Da) and the buffer was changed to phosphate buffer (20 mM, NaH₂PO₄/Na₂HPO₄) at pH 7.5 in D₂O.

El Tor CTB was prepared as previously described (Heggelund, Haugen, et al. 2012). Briefly, the protein was over-expressed in *Vibrio* sp. 60, grown in LBS medium (LB medium with 15g/l NaCl) 30 °C, 160 rpm, supplemented with 100 µl/ml ampicillin, until OD₆₀₀ reached 0.2. After induction with 0.5 mM IPTG, the cultures were grown for additional 16-20 h. The CTB is naturally secreted into the growth medium, and after removal of bacteria by centrifugation, the supernatant was purified by affinity chromatography. The protein was captured by the immobilized D-galactose gel (Thermo Scientific) and eluted using a galactose gradient. After dialysis against 0.1 M MES pH 6.0, the protein was further purified by ion exchange chromatography (HiTrap™ SP XL, GE Healthcare) using an NaCl gradient. Finally, the purified CTB was dialyzed against a storage buffer (20 mM Tris/HCl, 200 mM NaCl pH 7.5), and concentrated to 9.5 mg/ml. Prior to the NMR studies, the buffer was changed to phosphate buffer at pH 7.5 in D₂O, as described for classical CTB.

NMR experiments

Each sample was prepared in a 3 mm NMR tube using different ligand concentrations (from 1 mM to 20 mM) in the presence of 43 μ M or 46 μ M c CTB, depending on the experiment, or 34 μ M ET CTB, in 180 μ l of phosphate buffer (20 mM, $\text{NaH}_2\text{PO}_4/\text{Na}_2\text{HPO}_4$) at pH 7.5 in D_2O .

The spectra were acquired with a Bruker Avance 600 MHz instrument at 298 K. For the complete assignment of the molecules and the conformational analysis, the following experiments were used: 1D, COSY, TOCSY with a mixing time of 60 ms, NOESY with mixing times of 200 and 700 ms, $^1\text{H},^{13}\text{C}$ -HSQC ($J=145$ Hz). In the presence of an intense unwanted water signal at 4.7 ppm, solvent suppression was achieved by use of an excitation sculpting pulse sequence. The spectrum shows two set of signals (1:1 ratio) due to the presence of an equilibrium α/β anomeric mixture of the reducing end glucose.

The STD spectra were performed with an on-resonance irradiation frequency at -0.05 ppm or -0.5 ppm, while 200 ppm was chosen as off-resonance frequency. The experiments were performed at different temperatures (283 K to 298 K), but the best results were obtained at 298 K.

Selective presaturation of the protein was achieved by a train of Gauss shaped pulses, each of 49 ms in length. STD experiments were acquired with 0.98s or 2.94 s of total saturation times. The STD sequence was obtained from standard Bruker library and water suppression was achieved by using the WATERGATE 3–9–19 pulse sequence.

Funding. This work was supported by the Marie Curie Program [Contract DoubleLicht to AB and JJR , PIEF-GA-2009-251763] and by the University of Oslo.

1
2
3 **Acknowledgements.** We thank Timothy R. Hirst for providing us with the El Tor
4 CTB construct and the *Vibrio sp.* 60 expression host and Elicityl for a generous
5 discount on the purchase of the blood group antigen analogs.
6
7
8

9
10
11 **Abbreviations.** A-penta, blood group A pentasaccharide
12 GalNAc α 3[Fuc α 2]Gal β 4[Fuc α 3]Glc; B-penta, blood group B pentasaccharide
13 Gal α 3[Fuc α 2]Gal β 4[Fuc α 3]Glc; CT, cholera toxin; CTB, cholera toxin B-pentamer;
14 Gal α 3[Fuc α 2]Gal β 4[Fuc α 3]Glc; CT, cholera toxin; CTB, cholera toxin B-pentamer;
15 cCTB, classical cholera toxin B-pentamer; ET CTB, El Tor cholera toxin B-pentamer;
16 Fuc, L-fucose; Gal, D-galactose; GalNAc, 2'-N-acetyl D-galactosamine; Glc, D-
17 glucose, GlcNAc, 2'-N-acetyl D-glucosamine; GM1-os, oligosaccharide part of the
18 GM1 ganglioside, i.e. the Gal β 3GalNAc β 4[NeuAc α 3]Gal β 4Glc pentasaccharide; H-
19 tetra, blood group H tetrasaccharide Fuc α 2Gal β 4[Fuc α 3]Glc
20
21
22
23
24
25
26
27
28
29
30
31
32
33
34
35
36
37
38
39
40
41
42
43
44
45
46
47
48
49
50
51
52
53
54
55
56
57
58
59
60

REFERENCES.

- 1
2
3
4
5
6
7
8
9
10
11
12
13
14
15
16
17
18
19
20
21
22
23
24
25
26
27
28
29
30
31
32
33
34
35
36
37
38
39
40
41
42
43
44
45
46
47
48
49
50
51
52
53
54
55
56
57
58
59
60
- Ångström J, Bäckström M, Berntsson A, Karlsson N, Holmgren J, Karlsson K-A, Lebens M, Teneberg S. 2000. Novel carbohydrate binding site recognizing blood group A and B determinants in a hybrid of cholera toxin and *Escherichia coli* heat-labile enterotoxin B-subunits. *J Biol Chem*, 275:3231-3238.
- Angulo J, Díaz I, Reina JJ, Tabarani G, Fieschi F, Rojo J, Nieto PM. 2008. Saturation Transfer Difference (STD) NMR Spectroscopy Characterization of Dual Binding Mode of a Mannose Disaccharide to DC-SIGN. *ChemBioChem*, 9: 2225–2227.
- Angulo J, Enríquez-Navas PM, Nieto PM. 2010. Ligand-receptor binding affinities from saturation transfer difference (STD) NMR spectroscopy: the binding isotherm of STD initial growth rates. *Chem Eur J*, 16:7803-7812.
- Angulo J, Nieto PM. 2011. STD-NMR: application to transient interactions between biomolecules-a quantitative approach. *Eur Biophys J*, 40:1357-1369.
- Arifuzzaman M, Ahmed T, Rahman MA, Chowdhury F, Rashu R, Khan AI, LaRocque RC, Harris JB, Bhuiyan TR, Ryan ET, *et al.* 2011. Individuals with Le(a+b-) blood group have increased susceptibility to symptomatic *Vibrio cholerae* O1 infection. *PLoS Negl Trop Dis*, 5:e1413.
- Barua D, Paguio AS. 1977. ABO blood groups and cholera. *Ann Hum Biol*, 4:489-492.
- Bernardi A, Arosio D, Manzoni L, Monti D, Posteri H, Potenza D, Mari S, Jimenez-Barbero J. 2003. Mimics of ganglioside GM1 as cholera toxin ligands: replacement of the GalNAc residue. *Org Biomol Chem*, 1:785-792.
- Bhuiyan NA, Nusrin S, Alam M, Morita M, Watanabe H, Ramamurthy T, Cravioto A, Nair GB. 2009. Changing genotypes of cholera toxin (CT) of *Vibrio cholerae*

- 1
2
3 O139 in Bangladesh and description of three new CT genotypes. *FEMS Immunol*
4 *Med Microbiol*, 57:136-141.
5
6
7 Bhunia A, Bhattacharjya S, Chatterjee S. 2012. Applications of saturation transfer
8 difference NMR in biological systems. *Drug Discov Today*, 17:505-513.
9
10
11 Blank D, Dotz V, Geyer R, Kunz C. 2012. Human milk oligosaccharides and Lewis
12 blood group: individual high-throughput sample profiling to enhance conclusions
13 from functional studies. *Adv Nutr* 3:4405-95.
14
15
16 Chaudhuri A, De S. 1977. Cholera and blood-groups. *Lancet*, 310:404.
17
18
19 Chaudhuri A, DasAdhikary CR. 1978. Possible role of blood-group secretory
20 substances in the aetiology of cholera. *Trans R Soc Trop Med Hyg*, 72:664-665.
21
22
23 Clemens JD, Sack DA, Harris JR, Chakraborty J, Khan MR, Huda S, Ahmed F,
24 Gomes J, Rao MR, Svennerholm A-M, *et al.* 1989. ABO blood groups and
25 cholera: new observations on specificity of risk and modification of vaccine
26 efficacy. *J Infect Dis*, 159:770-773.
27
28
29 Dalvit C. 2009. NMR methods in fragment screening: theory and a comparison with
30 other biophysical techniques. *Drug Discov Today*, 14:1051-1057.
31
32
33
34 Glass RI, Holmgren J, Haley CE, Khan MR, Svennerholm A-M, Stoll BJ, Hossain
35 KMB, Black RE, Yunus M, Barua D. 1985. Predisposition for cholera of
36 individuals with O blood group. Possible evolutionary significance. *Am J*
37 *Epidemiol*, 121:791-796.
38
39
40
41 Harris JB, Khan AI, LaRocque RC, Dorer DJ, Chowdhury F, Faruque ASG, Sack
42 DA, Ryan ET, Qadri F, Calderwood SB. 2005. Blood group, immunity, and risk of
43 infection with *Vibrio cholerae* in an area of endemicity. *Infect Immun*, 73:7422-
44 7427.
45
46
47
48
49
50
51
52
53
54
55
56
57
58
59
60

- 1
2
3 Harris JB, LaRocque RC, Chowdhury F, Khan AI, Logvinenko T, Faruque ASG,
4 Ryan ET, Qadri F, Calderwood SB. 2008. Susceptibility to *Vibrio cholerae*
5 infection in a cohort of household contacts of patients with cholera in Bangladesh.
6 *PLoS Negl Trop Dis*, 2:e221.
7
8
9
10
11 Haselhorst T, Espinosa J-F, Jiménez-Barbero J, Sokolowski T, Kosma P, Brade H,
12 Brade L, Peters T. 1999. NMR experiments reveal distinct antibody-bound
13 conformations of a synthetic disaccharide representing a general structural element
14 of bacterial lipopolysaccharide epitopes. *Biochemistry*, 38:6449-6459.
15
16
17
18
19
20 Heggelund JE, Haugen E, Lygren B, Mackenzie A, Holmner Å, Vasile F, Reina JJ,
21 Bernardi A, Krenzel U. 2012. Both El Tor and classical cholera toxin bind blood
22 group determinants. *Biochem Biophys Res Commun*, 418:731-735.
23
24
25
26
27
28 Holmner Å, Lebens M, Teneberg S, Ångström J, Ökvist M, Krenzel U. 2004. Novel
29 binding site identified in a hybrid between cholera toxin and heat-labile
30 enterotoxin: 1.9 Å crystal structure reveals the details. *Structure*, 12:1655-1667.
31
32 (Erratum: *Structure* 2007. 15:253)
33
34
35
36
37 Holmner Å, Askarieh G, Ökvist M, Krenzel U. 2007. Blood group antigen
38 recognition by *Escherichia coli* heat-labile enterotoxin. *J Mol Biol*, 371:754-764.
39
40
41
42
43
44
45
46
47
48
49
50
51
52
53
54
55
56
57
58
59
60
- Mandal PK, Branson TR, Hayes ED, Ross JF, Gavín JA, Daranas AH, Turnbull WB.
2012. Towards a structural basis for the relationship between blood group and the
severity of El Tor cholera. *Angew Chem Int Ed*, 51:5143-5146.
- Mayer M, Meyer B. 1999. Characterization of ligand binding by saturation transfer
difference NMR spectroscopy. *Angew Chem Int Ed*, 38:1784-1788.
- Mayer M, Meyer B. 2000. Mapping the active site of angiotensin-converting enzyme
by transferred NOE spectroscopy. *J Med Chem*, 43:2093-2099.

- 1
2
3 Mayer M, Meyer B. 2001. Group epitope mapping by saturation transfer difference
4
5 NMR to identify segments of a ligand in direct contact with a protein receptor. *J*
6
7 *Am Chem Soc*, 123:6108-6117.
8
9
10 Mayer M, James TL. 2004. NMR-Based Characterization of Phenothiazines as a
11
12 RNA Binding Scaffold. *J Am Chem Soc*, 126: 4453-4460.
13
14 Merritt EA, Kuhn P, Sarfaty S, Erbe JL, Holmes RK, Hol WGJ. 1998. The 1.25 Å
15
16 resolution refinement of the cholera toxin B-pentamer: evidence of peptide
17
18 backbone strain at the receptor-binding site. *J Mol Biol*, 282:1043-1059.
19
20
21 Meyer B, Weimar T, Peters T. 1997. Screening mixtures for biological activity by
22
23 NMR. *Eur J Biochem*, 246:705-709.
24
25
26 Meyer B, Peters T. 2003. NMR spectroscopy techniques for screening and identifying
27
28 ligand binding to protein receptors. *Angew Chem Int Ed*, 42:864-890.
29
30
31 Nair GB, Qadri F, Holmgren J, Svennerholm A-M, Safa A, Bhuiyan NA, Ahmad QS,
32
33 Faruque SM, Faruque ASG, Takeda Y, *et al.* 2006. Cholera due to altered El Tor
34
35 strains of *Vibrio cholerae* O1 in Bangladesh. *J Clin Microbiol*, 44:4211-4213.
36
37
38 Newburg DS, Ruiz-Palacios GM, Altaye M, Chaturvedi P, Meinzen-Derr J, de
39
40 Lourdes Guerrero M, Morrow, AL. 2004. Innate protection conferred by
41
42 fucosylated oligosaccharides of human milk against diarrhea in breastfed infants.
43
44 *Glycobiology*, 14:253-63.
45
46
47 Nomenclature Committee, Consortium for Functional Glycomics. Symbol and text
48
49 nomenclature for representation of glycan structure. Available from
50
51 <http://www.functionalglycomics.org/static/consortium/Nomenclature.shtml>.
52
53 Accessed 2014 April 29.
54
55
56 Post CB. 2003. Exchange-transferred NOE spectroscopy and bound ligand structure
57
58 determination. *Curr Opin Struct Biol*, 13:581-588.
59
60

- 1
2
3 Ravn V, Dabelsteen E. 2000. Tissue distribution of histo-blood group antigens.
4
5 *APMIS*, 108:1-28.
6
7 Sánchez J, Holmgren J. 2008. Cholera toxin structure, gene regulation and
8
9 pathophysiological and immunological aspects. *Cell Mol Life Sci*, 65:1347-1360.
10
11 Swerdlow DL, Mintz ED, Rodriguez M, Tejada E, Ocampo C, Espejo L, Barrett TJ,
12
13 Petzelt J, Bean NH, Seminario L, *et al.* 1994. Severe life-threatening cholera
14
15 associated with blood group O in Peru: implications for the Latin American
16
17 epidemic. *J Infect Dis*, 170:468-472.
18
19
20
21 Turnbull WB, Precious BL, Homans SW 2004. Dissecting the cholera toxin-
22
23 ganglioside GM1 interaction by isothermal titration calorimetry. *J Am Chem Soc*,
24
25 126:1047-1054.
26
27
28 Yuriev E, Farrugia W, Scott AM, Ramsland PA. 2005. Three-dimensional structures
29
30 of carbohydrate determinants of Lewis system antigens: Implications for effective
31
32 antibody targeting of cancer. *Immunol Cell Biol*, 83:709–717.
33
34
35
36
37
38
39
40
41
42
43
44
45
46
47
48
49
50
51
52
53
54
55
56
57
58
59
60

LEGENDS TO FIGURES

Figure 1. Structures of the blood group antigen oligosaccharides **1-3** and the GM1 oligosaccharide **4** (GM1-os). Carbohydrate symbols follow the nomenclature of the Consortium for Functional Glycomics (Nomenclature committee, Consortium for Functional Glycomics, 2014); *N*-acetylneuraminic acid – purple diamond; D-galactose – yellow circle; *N*-acetylgalactosamine – yellow square; D-glucose – blue circle; *N*-acetylglucosamine – blue square; L-fucose – red triangle.

Figure 2. Absolute STD values and calculated K_d values for ABH antigen analogs. (A) H-tetra **1b** with classical CTB (cCTB) (blue bars) or El Tor CTB (ET) (grey bar). (B) A-penta **2b** with cCTB (red bars) or ET (grey bar). (C) B-penta **3b** with cCTB (green bars) or ET (grey bar). Note that the H5 Fuc(II) signal could not be analyzed in **3b**, due to overlap. Residues Fuc(I), Fuc(II), Gal and Gal(II) are defined in Figure 3. Only data for non-overlapping signals are reported.

Figure 3. Relative STD values, grouped in four intensity ranges, for antigen analogs H-tetra (**1b**), A-penta (**2b**) and B-penta (**3b**), interacting with both toxins.

Figure 4. H tetrasaccharide binding to cCTB. (A) STD (10240 transients and 2.94s of saturation time) and (B) ^1H -NMR spectrum of blood group H-tetrasaccharide **1b** (2.6 mM) in the presence of classical CTB (43 μM) (**1b**/cCTB 60:1).

Figure 5. H-tetra and GM1-os interact with cCTB simultaneously. (A) NOESY spectrum of H-tetra **1b** in phosphate buffer shows positive (red) cross peaks. (B) tr-

1
2
3 NOESY spectrum of H-tetra (0.9 mM) in the presence of cCTB, (43 μ M); negative
4
5 NOE contacts (black cross peaks) indicate binding. (C) tr-NOESY of H-tetra **1b** +
6
7 cCTB + GM1-os (**1b**/cCTB/GM1-os = 20:1:20) in buffer solution. The H-tetra cross
8
9 peaks are negative, showing that the blood group H antigen analog is not displaced
10
11 from its binding site. Negative cross peaks for GM1-os (yellow circles) indicate that
12
13 both compounds, H-tetra and GM1-os, interact with CTB simultaneously.
14
15
16
17

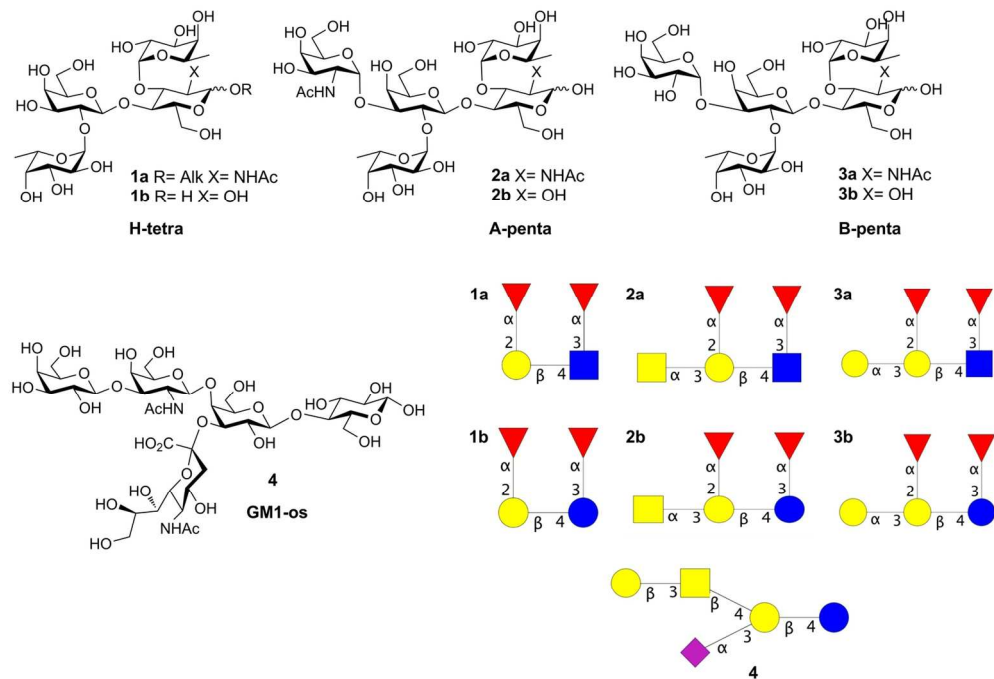
18
19 **Figure 6.** Simultaneous binding of H-tetra and GM1-os to cCTB confirmed by STD.

20
21 (A) 1 H-NMR spectrum of H-tetra **1b** (0.9 mM) in the presence of cCTB (43 μ M). (B)
22
23 1 H-NMR spectrum of **1b** (0.9 mM) and GM1-os **4** (0.9 mM) in the presence of cCTB
24
25 (43 μ M). The signals marked with an asterisk belong to GM1-os. (C) STD spectrum
26
27 (obtained with 10240 transients and 2.94s of saturation time) corresponding to (B).
28
29
30
31

32
33 **Figure 7.** Blood group A-pentasaccharide binding to the two CTB variants. (A) STD
34
35 spectrum (obtained with 10240 transients and 2.94s of saturation time) of A-penta **2b**
36
37 (2.6 mM) and cCTB (43 μ M) (60:1 ratio). (B) 1 H-NMR spectrum of **2b**. (C) STD
38
39 spectrum (10240 transients and 2.94s of saturation time) of A-penta **2b** (1.7 mM) and
40
41 ET CTB (34 μ M) (50:1 ratio); the signals marked with an asterisk are artifacts.
42
43
44
45

46
47 **Figure 8.** Blood group B-pentasaccharide binding to the two CTB variants. (A) STD
48
49 spectrum (obtained with 10240 transients and 2.94s of saturation time) of B-penta **3b**
50
51 (2.0 mM) and cCTB (46 μ M) (45:1 ratio). (B) 1 H-NMR spectrum of **3b**. (C) STD
52
53 spectrum (10240 transients and 2.94s of saturation time) of B-penta **3b** (1.7 mM) and
54
55 ET CTB (34 μ M) (50:1 ratio); the signals marked with an asterisk are artifacts.
56
57
58
59
60

1
2
3 **Figure 9.** Modeled antigen interactions. (A) Close-up view of the A-pentasaccharide
4 **2b** bound to CTB, showing the relative STD intensity values for the interaction with
5 cCTB (from Figure 3) as colored dots. The ligand and selected amino acid residues
6 are given in stick representation, while the protein is shown as a surface
7 representation (with different colors for the individual B-subunits). The figure was
8 generated based on the crystal structures of classical CTB (PDB ID: 3CHB, Merritt,
9 Kuhn, et al. 1998) and the ligand complex of a CTB/LTB chimera (PDB ID: 3EFX,
10 Holmner, Lebens, et al. 2004). The two residues differing between classical and El
11 Tor CTB are shown in purple (classical) and green (El Tor), with Ile47 being
12 introduced manually in its preferred rotamer conformation (Insert: collage of CTB
13 binding to the A-pentasaccharide (light grey) and GM1-os (turquoise)). (B) Stereo
14 representation of A, including the water molecules of the A-penta complex (PDB ID:
15 3EFX, Holmner, Lebens, et al. 2004), and their H-bond of the blood group
16 determinant is opposite to the conventional orientation shown in Figure 1, since CTB
17 is displayed in its standard view, with the GM1 binding site facing down towards the
18 cell surface.
19
20
21
22
23
24
25
26
27
28
29
30
31
32
33
34
35
36
37
38
39
40
41
42
43
44
45
46
47
48
49
50
51
52
53
54
55
56
57
58
59
60



30 Figure 1. Structures of the blood group antigen oligosaccharides 1-3 and the GM1 oligosaccharide 4 (GM1-
31 os). Carbohydrate symbols follow the nomenclature of the Consortium for Functional Glycomics
32 (Nomenclature committee, Consortium for Functional Glycomics, 2014); N-acetylneuraminic acid – purple
33 diamond; D-galactose – yellow circle; N-acetylgalactosamine – yellow square; D-glucose – blue circle; N-
34 acetylglucosamine – blue square; L-fucose – red triangle.
35 142x97mm (300 x 300 DPI)

36
37
38
39
40
41
42
43
44
45
46
47
48
49
50
51
52
53
54
55
56
57
58
59
60

Review

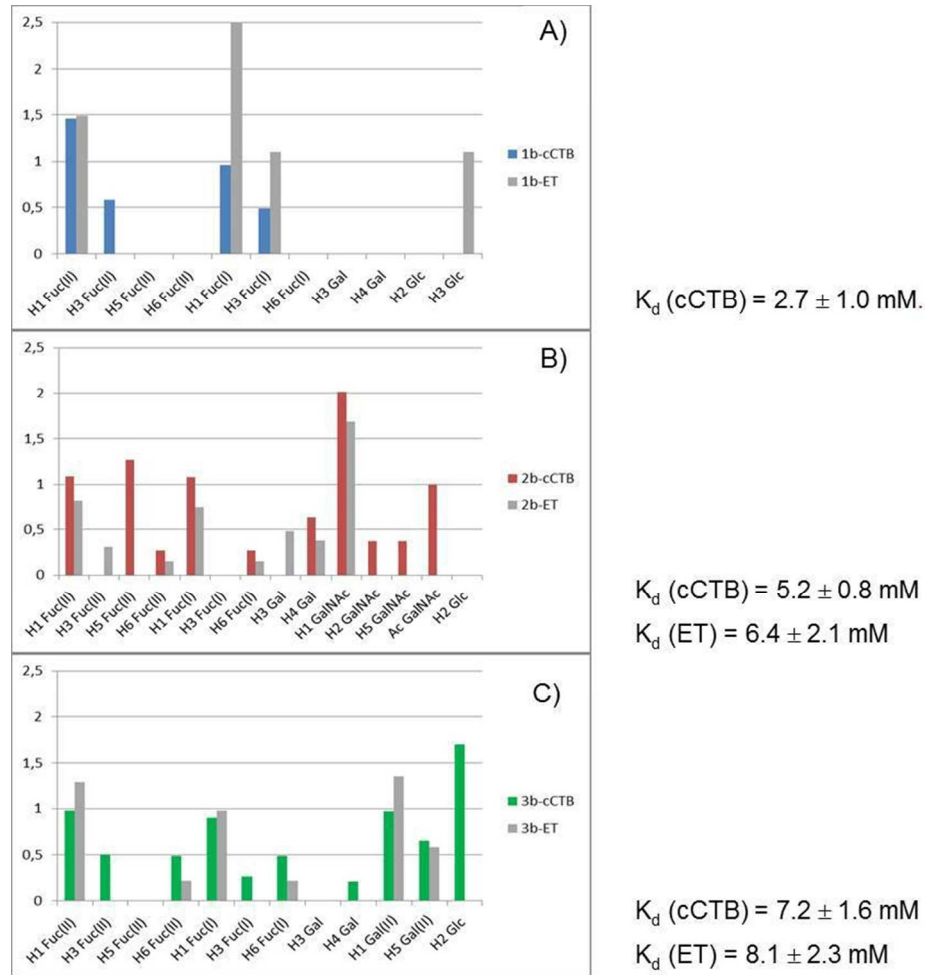
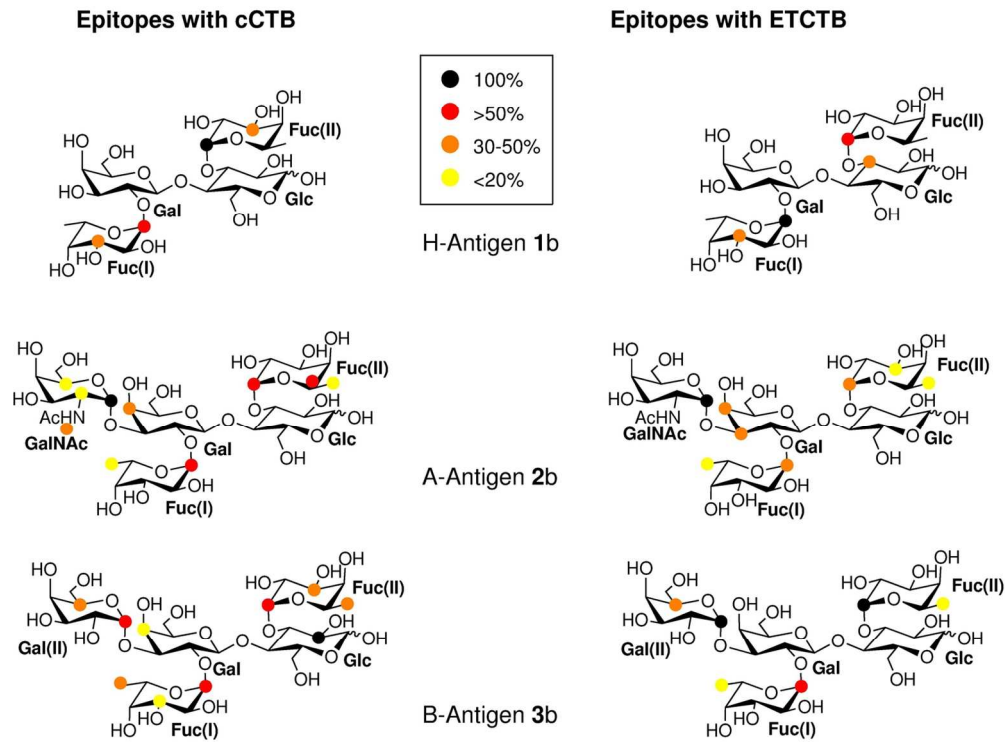


Figure 2. Absolute STD values and calculated K_d values for ABH antigen analogs. (A) H-tetra 1b with classical CTB (cCTB) (blue bars) or El Tor CTB (ET) (grey bar). (B) A-penta 2b with cCTB (red bars) or ET (grey bar). (C) B-penta 3b with cCTB (green bars) or ET (grey bar). Note that the H5 Fuc(II) signal could not be analyzed in 3b, due to overlap. Residues Fuc(I), Fuc(II), Gal and Gal(II) are defined in Figure 3. Only data for non-overlapping signals are reported.

77x75mm (300 x 300 DPI)



32 Figure 3. Relative STD values, grouped in four intensity ranges, for antigen analogs H-tetra (1b), A-penta
33 (2b) and B-penta (3b), interacting with both toxins.
34 134x99mm (300 x 300 DPI)

35
36
37
38
39
40
41
42
43
44
45
46
47
48
49
50
51
52
53
54
55
56
57
58
59
60

review

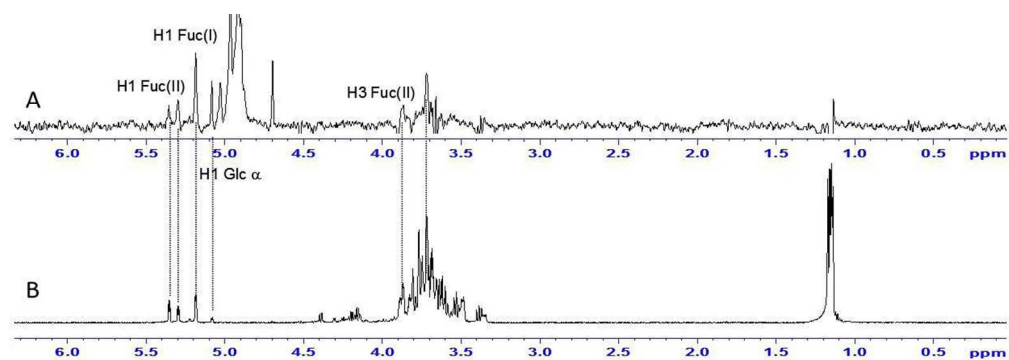
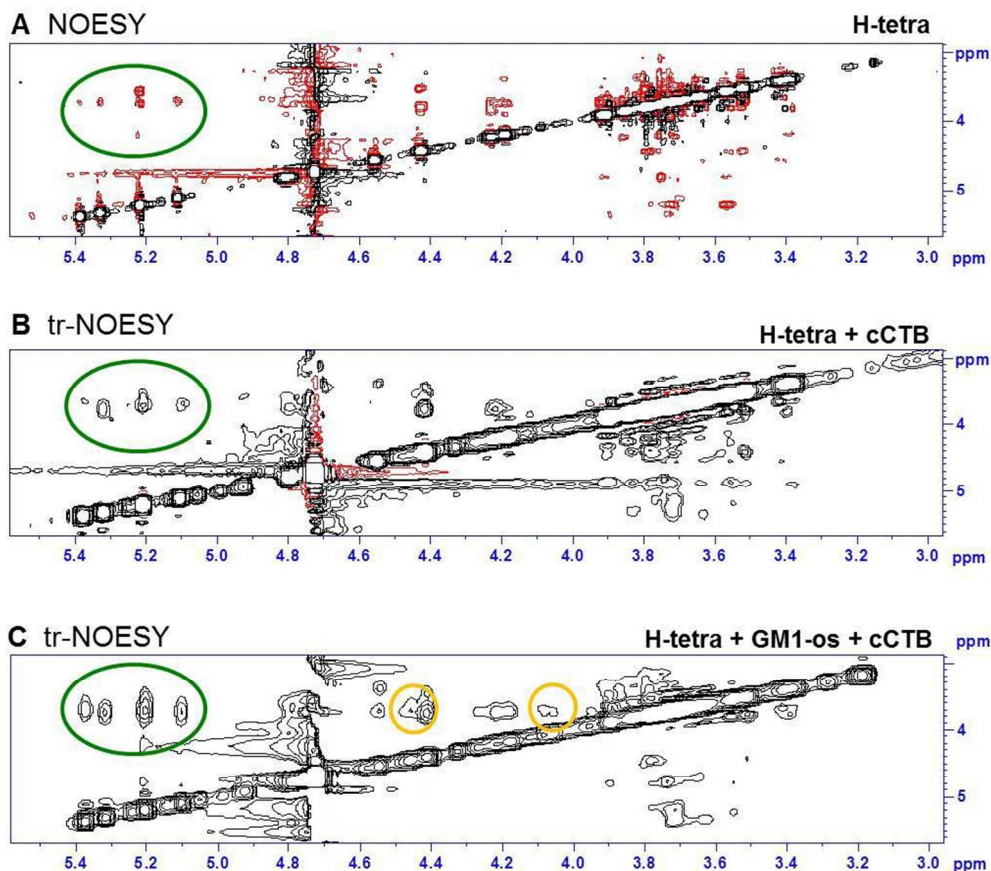


Figure 4. H tetrasaccharide binding to cCTB. (A) STD (10240 transients and 2.94s of saturation time) and (B) ^1H -NMR spectrum of blood group H-tetrasaccharide 1b (2.6 mM) in the presence of classical CTB (43 μM) (1b/cCTB 60:1).
105x38mm (300 x 300 DPI)

Peer Review



36
37
38
39
40
41
42
43
44
45
46
47
48
49
50
51
52
53
54
55
56
57
58
59
60

Figure 5. H-tetra and GM1-os interact with cCTB simultaneously. (A) NOESY spectrum of H-tetra 1b in phosphate buffer shows positive (red) cross peaks. (B) tr-NOESY spectrum of H-tetra (0.9 mM) in the presence of cCTB, (43 μ M); negative NOE contacts (black cross peaks) indicate binding. (C) tr-NOESY of H-tetra 1b + cCTB + GM1-os (1b/cCTB/GM1-os = 20:1:20) in buffer solution. The H-tetra cross peaks are negative, showing that the blood group H antigen analog is not displaced from its binding site. Negative cross peaks for GM1-os (yellow circles) indicate that both compounds, H-tetra and GM1-os, interact with CTB simultaneously.

86x75mm (300 x 300 DPI)

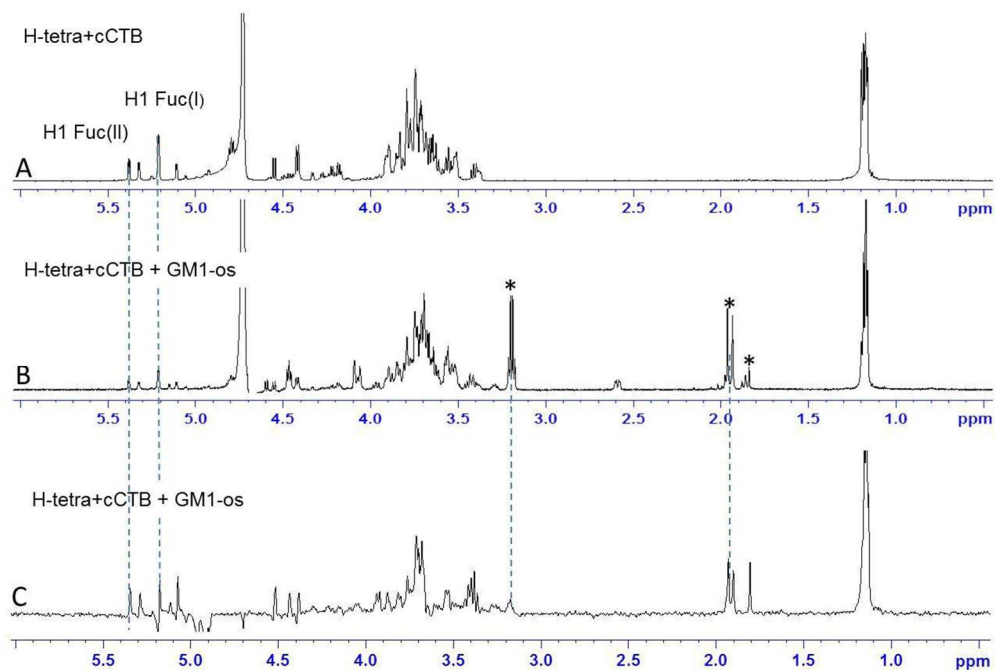


Figure 6. Simultaneous binding of H-tetra and GM1-os to cCTB confirmed by STD. (A) ¹H-NMR spectrum of H-tetra 1b (0.9 mM) in the presence of cCTB (43 μ M). (B) ¹H-NMR spectrum of 1b (0.9 mM) and GM1-os 4 (0.9 mM) in the presence of cCTB (43 μ M). The signals marked with an asterisk belong to GM1-os. (C) STD spectrum (obtained with 10240 transients and 2.94s of saturation time) corresponding to (B).
108x79mm (300 x 300 DPI)

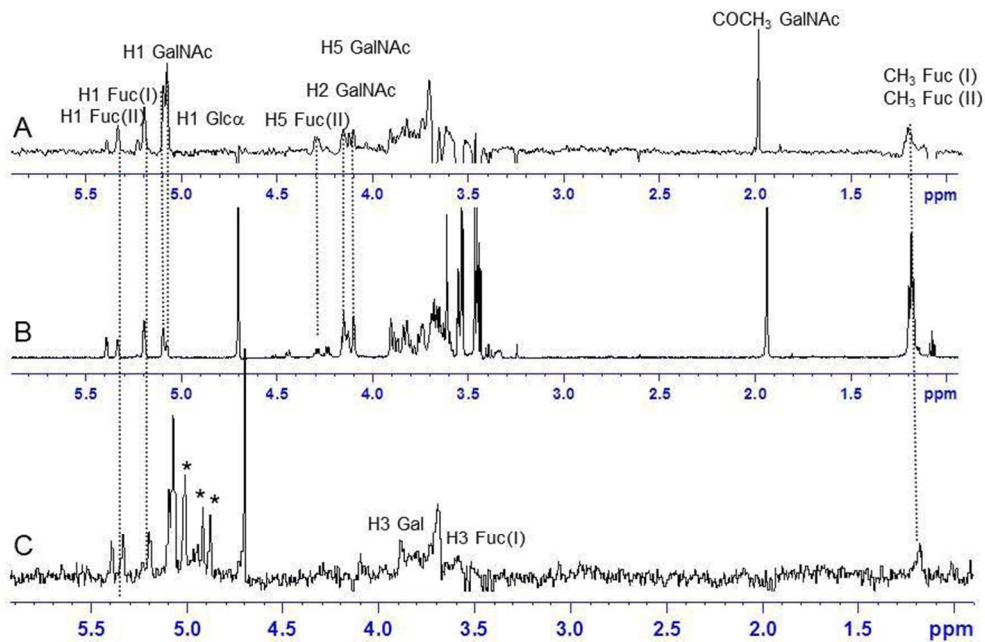


Figure 7. Blood group A-pentasaccharide binding to the two CTB variants. (A) STD spectrum (obtained with 10240 transients and 2.94s of saturation time) of A-penta 2b (2.6 mM) and cCTB (43 μM) (60:1 ratio). (B) $^1\text{H-NMR}$ spectrum of 2b. (C) STD spectrum (10240 transients and 2.94s of saturation time) of A-penta 2b (1.7 mM) and ET CTB (34 μM) (50:1 ratio); the signals marked with an asterisk are artifacts.
75x48mm (300 x 300 DPI)

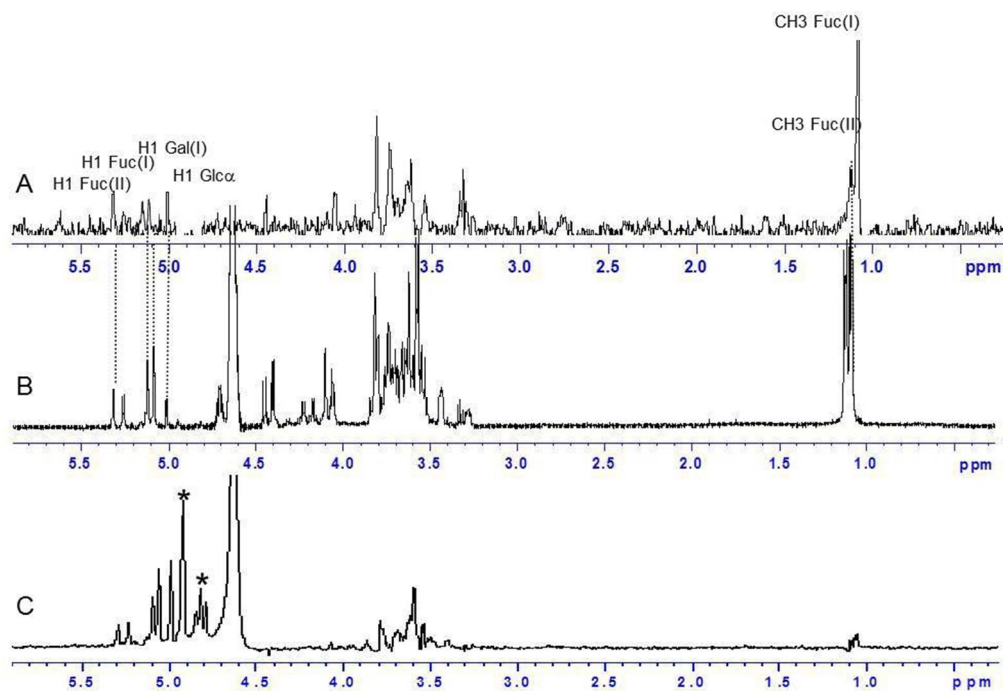


Figure 8. Blood group B-pentasaccharide binding to the two CTB variants. (A) STD spectrum (obtained with 10240 transients and 2.94s of saturation time) of B-penta 3b (2.0 mM) and cCTB (46 μM) (45:1 ratio). (B) 1H-NMR spectrum of 3b. (C) STD spectrum (10240 transients and 2.94s of saturation time) of B-penta 3b (1.7 mM) and ET CTB (34 μM) (50:1 ratio); the signals marked with an asterisk are artifacts.
82x56mm (300 x 300 DPI)

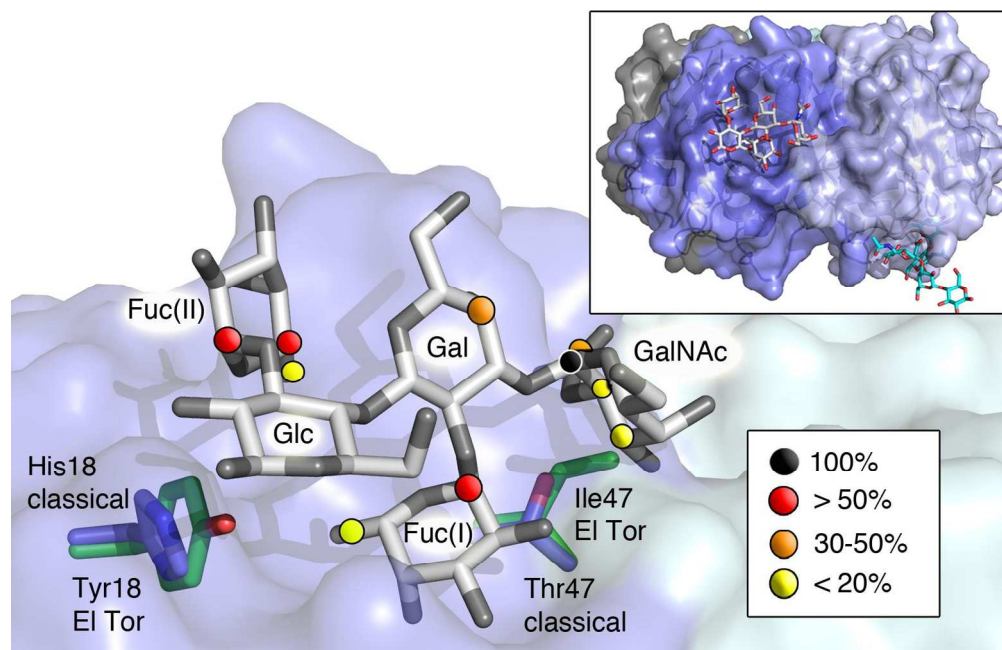


Figure 9. Modeled antigen interactions. (A) Close-up view of the A-pentasaccharide 2b bound to CTB, showing the relative STD intensity values for the interaction with cCTB (from Figure 3) as colored dots. The ligand and selected amino acid residues are given in stick representation, while the protein is shown as a surface representation (with different colors for the individual B-subunits). The figure was generated based on the crystal structures of classical CTB (PDB ID: 3CHB, Merritt, Kuhn, et al. 1998) and the ligand complex of a CTB/LTB chimera (PDB ID: 3EFX, Holmner, Lebens, et al. 2004). The two residues differing between classical and El Tor CTB are shown in purple (classical) and green (El Tor), with Ile47 being introduced manually in its preferred rotamer conformation (Insert: collage of CTB binding to the A-pentasaccharide (light grey) and GM1-os (turquoise)).

623x402mm (72 x 72 DPI)

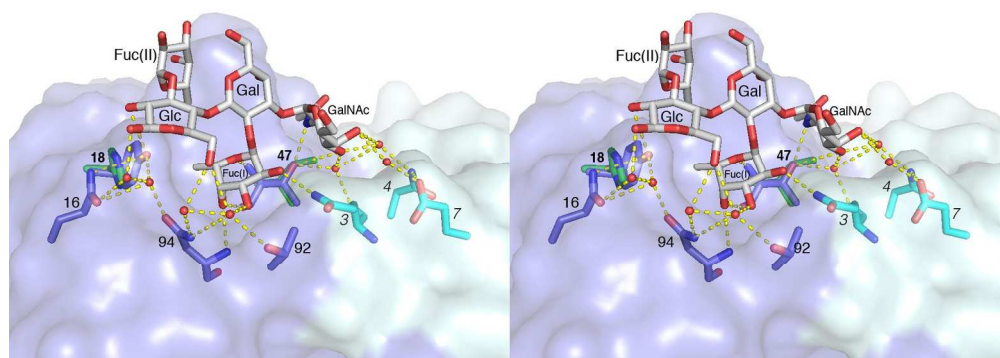


Figure 9. (B) Stereo representation of A, including the water molecules of the A-penta complex (PDB ID: 3EFX, Holmner, Lebens, et al. 2004), and their H-bonding interactions. Note that the orientation of the blood group determinant is opposite to the conventional orientation shown in Figure 1, since CTB is displayed in its standard view, with the GM1 binding site facing down towards the cell surface.

705x282mm (72 x 72 DPI)